

Surface-mediated self-assembly of click-reactive cello-oligosaccharides for fabricating functional nonwoven fabrics

Yudai Mizuuchi, Yuuki Hata , Toshiki Sawada  and Takeshi Serizawa 

Department of Chemical Science and Engineering, School of Materials and Chemical Technology, Tokyo Institute of Technology, Tokyo, Japan

ABSTRACT

Polymer fabrics are versatile materials used in various fields. Surface modification methods for hydrophobic polymer fibers have been developed to endow the materials with water wettability and functionality. Nevertheless, it remains a challenge to freely introduce functional groups to polymer fiber surfaces in a simple manner. Herein, we report the decoration of nonwoven fabric surfaces with azidated cello-oligosaccharide assemblies via molecular self-assembly. Cello-oligosaccharides with a terminal azido group were enzymatically synthesized and allowed to self-assemble in polyolefin, polyester, and vinylon nonwoven fabrics. It was found that the functional oligosaccharides formed bark-like assemblies on the nonwoven fiber surfaces, probably through heterogeneous nucleation. The hydrophilic oligosaccharide assemblies made the hydrophobic nonwoven surfaces water-wettable. Moreover, the azido group at oligosaccharide terminal was available for the post-functionalization of the modified nonwovens. In fact, an antigen was successfully conjugated to the modified nonwovens via the click chemistry. The antigen-conjugated nonwovens were useful for the specific and quantitative detection of a corresponding antibody. Our findings demonstrate the great potential of cello-oligosaccharide assembly for the functionalization of fabrics and other polymeric materials.

IMPACT STATEMENT

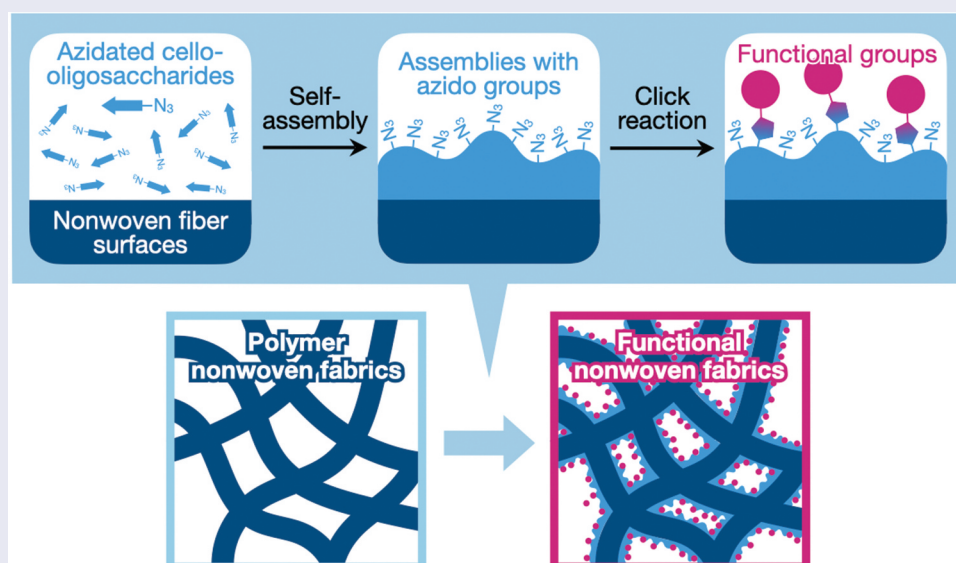
This study developed a novel and simple method for modifying surfaces of polymer nonwoven fabrics based on the self-assembly of azidated cello-oligosaccharides to fabricate water-wettable and click-reactive functional materials.

ARTICLE HISTORY

Received 20 December 2023
Accepted 23 January 2024
Revised 22 January 2024

KEYWORDS



Azidated cello-oligosaccharides; biomolecular sensing; nonwoven fabrics; surface-mediated self-assembly; water wettability




1. Introduction

Polymer fabrics are an important class of materials used in various applications, ranging from polymer composites to healthcare and electronic devices [1–6].

Representative synthetic polymers used in fabrics include polypropylene and polyethylene terephthalate, which are hydrophobic. The hydrophobicity of polymers endows fabrics with stability in humid and

CONTACT Takeshi Serizawa  serizawa@mac.titech.ac.jp  Department of Chemical Science and Engineering, School of Materials and Chemical Technology, Tokyo Institute of Technology, 2-12-1 Ookayama, Meguro-ku, Tokyo 152-8550, Japan

 Supplemental data for this article can be accessed online at <https://doi.org/10.1080/14686996.2024.2311052>.

© 2024 The Author(s). Published by National Institute for Materials Science in partnership with Taylor & Francis Group.

This is an Open Access article distributed under the terms of the Creative Commons Attribution-NonCommercial License (<http://creativecommons.org/licenses/by-nc/4.0/>), which permits unrestricted non-commercial use, distribution, and reproduction in any medium, provided the original work is properly cited. The terms on which this article has been published allow the posting of the Accepted Manuscript in a repository by the author(s) or with their consent.

aqueous environments. Nevertheless, hydrophobicity leads to low surface wettability with water, even though wettability is important for biomedical and other applications [7–9]. Meanwhile, applications in other fields, such as oil – water separation and self-cleaning, require polymer fabrics with superhydrophobic surfaces [8,10,11]. Thus, surface modification methods for hydrophobic polymer fabrics have been developed to alter surface hydrophilicity/hydrophobicity and, moreover, to introduce functional groups to fiber surfaces [12–15]. One of the most widely used methods is plasma treatment, which degrades polymers to generate hydrophilic groups (e.g. hydroxy group) on fiber surfaces [12]. Hydrophilic groups are available for covalently introducing functional groups to the fiber surfaces. Meanwhile, the physical adsorption of adhesive polymers [16], metal oxides [17], metal organic frameworks [18], and polymer crystals [19] has been investigated as a simple method. The physical adsorption approach has been shown to be useful for increasing surface wettability and further functionalization. Nevertheless, the free and stable introduction of functional groups to polymer fiber surfaces via physical adsorption remains a challenge.

Cello-oligosaccharides are emerging self-assembling building blocks for creating advanced materials with robustness and inertness [20,21]. Compared with other biomolecular assemblies, cello-oligosaccharide assemblies exhibit exceptional properties, such as solvent resistance, thermal stability, antibiofouling properties, and cytocompatibility [20]. These unique properties make those materials useful for nanomaterial confinement [22–24], interface stabilization [25–27], cell culture [28,29], nanocomposites [30], antibody detection [31], and biocompatible bactericidal action [32]. We recently demonstrated that cello-oligosaccharides self-assembled onto cellulose paper surfaces to form nanostructures

[33,34]. Notably, cello-oligosaccharide derivatives with terminal functional groups could be used as well; the self-assembly of cello-oligosaccharides with a terminal azido group enabled us to introduce the click-reactive group onto paper surfaces for subsequent conjugation of an antigen via Huisgen cycloaddition [33]. Analyses for the paper surface modification suggested that the self-assembly of cello-oligosaccharides into nanostructures occurred through heterogeneous nucleation on paper fiber surfaces rather than through epitaxial growth. This plausible assembly mechanism through heterogeneous nucleation, which does not rely on specific cellulose – cello-oligosaccharide interactions, implies that the surface modification by click-reactive cello-oligosaccharides will be applicable not only to cellulose materials but also to synthetic polymer fabrics.

Herein, we report the surface-mediated self-assembly of click-reactive cello-oligosaccharides on polymeric nonwoven surfaces (Figure 1). Cello-oligosaccharides with a terminal azido group were synthesized via the cellodextrin phosphorylase (CDP)-catalyzed oligomerization of α -D-glucose 1-phosphate (α G1P) monomers from 2-azidoethyl β -D-glucopyranoside primers. The synthesized click-reactive cello-oligosaccharides were dissolved in aqueous sodium hydroxide (NaOH) solutions and then applied to polyolefin, polyester, and vinylon nonwoven fabrics impregnated with isopropyl alcohol (IPA) aqueous solutions containing hydrogen chloride (HCl). The neutralization of alkaline solutions by HCl triggered the self-assembly of azidated cello-oligosaccharides. It was found that the oligosaccharide molecules successfully formed assemblies on nonwoven fiber surfaces. This result demonstrates that azidated cello-oligosaccharides can self-assemble onto materials surfaces via heterogeneous nucleation, although our previous report using paper left open the possibility that the self-assembly occurred via epitaxial growth. The

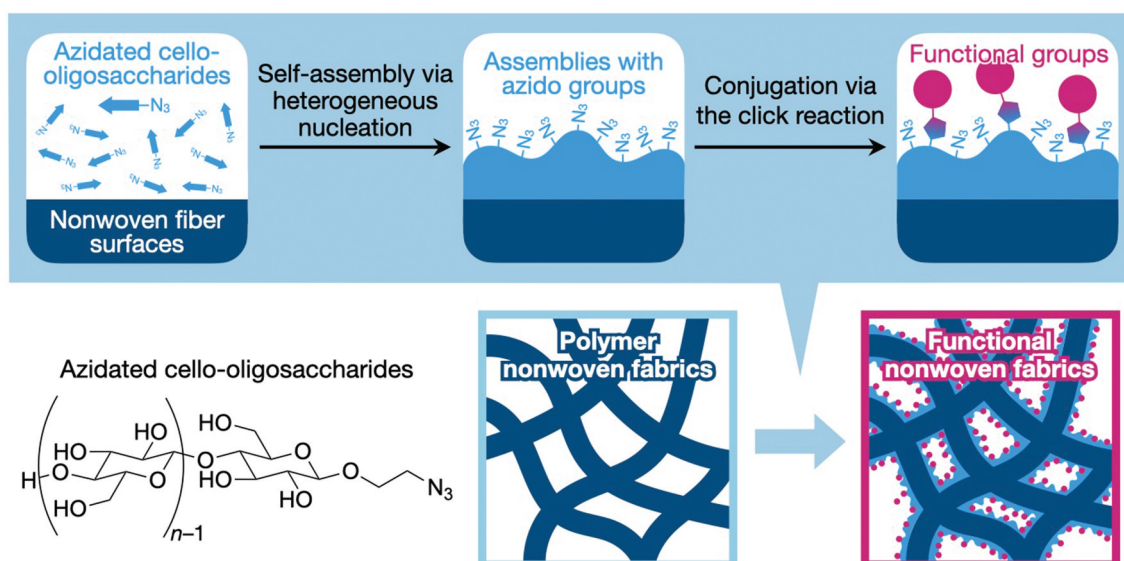


Figure 1. Schematic illustration of this study.

resultant surface-modified nonwovens were characterized by scanning electron microscopy (SEM), infrared absorption spectroscopy, and contact angle measurements. Moreover, azido groups on the nonwoven surfaces were chemically conjugated with an antigen via the click reactions to investigate the potential diagnostic applications of the modified nonwovens.

2. Materials and methods

2.1. Materials

2-Azidoethyl β -D-glucopyranoside and *N*-[(1*R*,8*S*,9*S*)-bicyclo[6.1.0]non-4-yn-9-ylmethylxycarbonyl]-1,8-diamino-3,6-dioxaoctane (BCN-amine) were purchased from Tokyo Chemical Industry (Tokyo, Japan). α G1P disodium salt *n*-hydrate was purchased from Nacalai Tesque (Kyoto, Japan) or Wako Pure Chemical Industries (Osaka, Japan). Acetonitrile, dimethyl sulfoxide (DMSO, dehydrated), potassium chloride, 4-(4,6-dimethoxy-1,3,5-triazin-2-yl)-4-methylmorpholinium (DMT-MM) chloride *n*-hydrate, bovine serum albumin (BSA, protease free), and 40% sodium deuterioxide (NaOD)/deuterium oxide (D₂O) solution were purchased from Wako Pure Chemical Industries (Osaka, Japan). 2,5-Dihydroxybenzoic acid, ProteoMass MALDI-MS Standards (Bradykinin fragment 1–7, P₁₄R, and ACTH fragment 18–39), 1% trifluoroacetic acid, D₂O, and horseradish peroxidase (HRP)-conjugated anti-mouse immunoglobulin G (IgG) IgG (produced in rabbits, polyclonal, lot: 0000143670) were purchased from Sigma – Aldrich (Missouri, U.S.A.). HRP-conjugated anti-biotin IgG (produced in rabbit, polyclonal, lot: A150-109P-19) was purchased from Bethyl Laboratories (Texas, U.S.A.). 31% hydrogen peroxide (H₂O₂) solution was purchased from Santoku Chemical Industries (Tokyo, Japan). All of the other reagents were purchased from Nacalai Tesque (Kyoto, Japan). Polyolefin nonwoven fabrics (HOP), polyester nonwoven fabrics (TH), and vinylon nonwoven fabrics (VN) were manufactured by Hirose Paper Mfg (Kochi, Japan). CDP derived from *Acetivibrio thermocellus* DSM 1313 with fused His-tag was expressed in *Escherichia coli* BL21-Gold (DE3) and purified using a Ni-NTA column [35]. Ultrapure water at more than 18.2 M Ω -cm was obtained from a Milli-Q Advantage A-10 (Merck Millipore) and used throughout the study.

2.2. Enzyme-catalyzed synthesis of oligosaccharides

The enzymatic synthesis of cello-oligosaccharides and azidated cello-oligosaccharides were performed according to the procedures described in our previous report (Figure S1) [33]. Briefly, 200 mM α G1P monomers and 50 mM primers (2-azidoethyl β -D-glucopyranoside or cellobiose) were mixed with

CDP (1 U mL⁻¹) in 500 mM 4-(2-hydroxyethyl)-1-piperazineethanesulfonic acid buffer solutions (pH 7.5) and incubated at 60°C for 3 days.

The produced water-insoluble oligosaccharides were purified with ultrapure water through at least five centrifugation (20,400 g)/redispersion cycles to remove 99.999% of the reaction solution. The purified oligosaccharides were dried at 105°C for 24 h and weighed to estimate the yields. Monomer conversions were calculated from the yields and the average degree of polymerization (DP) estimated by ¹H nuclear magnetic resonance (NMR) spectroscopy. The purified oligosaccharides were lyophilized and stored in a desiccator until further use.

2.3. Self-assembly of oligosaccharides in bulk solutions

Azidated cello-oligosaccharides or cello-oligosaccharides was dispersed at 2.67% (w/v) in 1.33 M NaOH aqueous solutions at room temperature, followed by dissolution at –20°C for 20 min. Then, 112.5 μ L of the oligosaccharides/NaOH aqueous solutions were mixed with 37.5 μ L of IPA and 150 μ L of 1 M HCl aqueous solutions containing 71.5 mM sodium dihydrogenphosphate and 58.5 mM disodium hydrogen phosphate (phosphate buffer species) before incubation at 25°C for 1 h. The self-assembled oligosaccharides were purified with ultrapure water through at least five centrifugation (20,400 g)/redispersion cycles. The purified dispersions were used for matrix-assisted laser desorption/ionization time-of-flight (MALDI-TOF) mass spectrometry as described below. The dispersions were lyophilized to obtain powder for ¹H NMR spectroscopy and attenuated total reflection-Fourier transform infrared (ATR-FTIR) absorption spectroscopy.

2.4. Characterizations of oligosaccharides

For ¹H NMR spectroscopy, the lyophilized cello-oligosaccharides were dissolved at more than 2.5% (w/v) in 4% NaOD/D₂O. The spectra were recorded using an AVANCE III HD spectrometer (500 MHz, Bruker Biospin, Massachusetts, U.S.A.) at room temperature and calibrated using residual water signals (δ = 4.79) as an internal standard. For MALDI-TOF mass spectrometry, 6 μ L of the never-dried cello-oligosaccharide dispersions (0.05% (w/v)) was mixed with 6 μ L of 2,5-dihydroxybenzoic acid (10 mg mL⁻¹), 3 μ L of trifluoroacetic acid (1% (v/v)), and 15 μ L of acetonitrile. The mixtures were deposited onto a sample target plate and dried in air. Mass spectra were recorded at room temperature using an AXIMA-performance mass spectrometer (Shimadzu, Kyoto, Japan) equipped with a nitrogen laser (λ = 337 nm) and pulsed ion extraction at an accelerating potential of 20 kV in linear/positive

ion mode. Peptide standards of 757.3997 Da (Bradykinin fragment 1–7), 1533.8582 Da (P₁₄R), and 2465.1989 Da (ACTH fragment 18–39) were used to calibrate the spectra. For ATR-FTIR absorption spectroscopy, an FT/IR-4100 spectrometer (JASCO, Tokyo, Japan) was operated at a cumulative number of 100 and a resolution of 2.0 cm⁻¹ for lyophilized oligosaccharides at room temperature.

For SEM observations, gels produced by the self-assembly of azidated cello-oligosaccharides were immersed in an IPA – ultrapure water mixture (1/7, v/v) for 10 days at 4°C. The IPA – ultrapure water mixture was exchanged every day. The resultant purified gels were sequentially immersed in 20, 30, 40, 50, 60, 70, 80, and 90% IPA, IPA, IPA-*tert*-butyl alcohol (1/1, v/v), and *tert*-butyl alcohol at room temperature. The resultant organogels were frozen in liquid nitrogen, fractured using a razor blade, and lyophilized. The lyophilized gels were adhered with Dotite to substrates and coated with osmium. A JSM-7500F field-emission scanning electron microscope (JEOL, Tokyo, Japan) was used to observe the fractured surfaces at an accelerating voltage of 5 kV.

2.5. Self-assembly of oligosaccharides in nonwovens

Nonwoven fabrics (1 cm in diameter) were immersed in 1 mL of IPA at 25°C for 1 h and dried on filter paper in air for 5 min. Typically, 2.5 μL of IPA, 10 μL of 1 M HCl aqueous solutions containing the phosphate buffer species, and 7.5 μL of 1.33 M NaOH aqueous solutions containing oligosaccharides were sequentially applied to the dried nonwovens and incubated at 25°C for 1 h. The resultant conditions for oligosaccharide assembly were 12.5% (v/v) IPA, 500 mM NaCl, and 1% (w/v) oligosaccharides unless otherwise stated.

To estimate the loading rates of cello-oligosaccharides to nonwovens, the nonwoven fabrics with self-assembled oligosaccharides were washed with 1 mL of a DMSO – ultrapure water mixture (1/1, v/v) by pipetting 10 times, and the first washings were collected. Then, the nonwoven fabrics were flipped and washed with 1 mL of a DMSO – ultrapure water mixture (1/1, v/v) again, and the second washings were collected. Optical densities of the first and second washings (OD_{1st washing} and OD_{2nd washing}, respectively) after 2-fold dilution were recorded at 500 nm using a V-670 ultraviolet – visible spectrometer (JASCO, Tokyo, Japan) at room temperature. The loading rates of oligosaccharides to nonwoven fabrics were estimated using the following equation:

$$(\% \text{Loading rate}) = \left[1 - \frac{(\text{OD}_{1\text{st washing}}) + (\text{OD}_{2\text{nd washing}})}{(\text{OD}_{\text{total oligosaccharides}})} \right] \times 100$$

where OD_{total oligosaccharides} indicates the OD of the oligosaccharide dispersions prepared through self-

assembly at 1% (w/v) in bulk solutions and subsequent dilution with a DMSO – ultrapure water mixture.

2.6. Characterizations of nonwovens with oligosaccharides

For SEM and ATR-FTIR absorption spectroscopy, the nonwoven fabrics with self-assembled oligosaccharides were sequentially immersed in 1 mL of 50, 60, 70, 80, and 90% ethanol, ethanol, ethanol-*tert*-butyl alcohol (1/1, v/v), and *tert*-butyl alcohol at room temperature. The resultant nonwoven fabrics impregnated with *tert*-butyl alcohol were lyophilized, adhered with carbon tape to substrates, and coated with osmium. The surfaces of nonwovens were observed using a JSM-7500F field-emission scanning electron microscope at an accelerating voltage of 5 kV. FTIR absorption spectra were recorded using an FT/IR-4100 spectrometer at a cumulative number of 100 and a resolution of 2.0 cm⁻¹.

For contact angle measurements, the nonwoven fabrics with self-assembled oligosaccharides were washed twice with ultrapure water by pipetting and dried overnight at 25°C in air. A water droplet (1 μL) was mounted onto the dried nonwoven surfaces using a contact angle meter (DMS-401, Kyowa Interfacial Science, Saitama, Japan). The contact angles after 100 ms were analyzed using FAMES analysis software (Kyowa Interfacial Science, Saitama, Japan) using the tangent method.

2.7. Conjugation of biotin to azidated cello-oligosaccharides in nonwovens

The nonwoven fabrics with self-assembled azidated cello-oligosaccharides were washed through immersion five times in a DMSO – phosphate-buffered saline (PBS: 137 mM sodium chloride, 8.2 mM disodium hydrogen phosphate, 2.7 mM potassium chloride, and 1.5 mM potassium dihydrogen phosphate) mixture (1/1, v/v) at room temperature. Clickable biotin was synthesized by incubating 48 mM biotin with 48 mM DMT-MM and 24 mM BCN-amine in a DMSO – PBS mixture at 25°C for 2 h. The resultant solutions containing clickable biotin were appropriately diluted with a DMSO – PBS mixture, and 500 μL of the diluted solutions was applied to the nonwovens impregnated with DMSO – PBS before incubation at 25°C for 1 h for the Huisgen cycloaddition reaction. The amount of clickable biotin molecules was 2-fold of that of the azidated cello-oligosaccharide molecules in nonwovens. Then, the biotin-conjugated nonwovens were washed with DMSO by immersion five times to remove unreacted species.

To calculate the conjugation rate of biotin to azidated cello-oligosaccharides in nonwovens, the biotin-conjugated nonwovens were washed five times with

ultrapure water by immersion and dried overnight at 25°C in air. To extract the oligosaccharides, the dried nonwovens were placed on a nylon mesh and impregnated with 10 μL of IPA and 30 μL of 1 M NaOH aqueous solutions to extract oligosaccharides for 3 min. The solutions containing dissolved oligosaccharides were collected by centrifugation at 5,000 g. Then, 10 μL of IPA and 20 μL of 1 M NaOH aqueous solutions were added to the nonwovens after centrifugation, and the solutions containing dissolved oligosaccharides were collected by centrifugation at 5,000 g. The collected alkaline solutions containing oligosaccharides were neutralized with 6 M HCl and left to stand at 25°C for 3 h. The precipitated oligosaccharides were purified with ultrapure water by five centrifugation/redispersion cycles and subjected to MALDI-TOF mass spectrometry measurements. The conjugation rate was calculated based on the peak areas of unreacted azidated cello-oligosaccharides and biotin-conjugated cello-oligosaccharides in the mass spectra.

2.8. Detection of HRP-conjugated IgGs using nonwovens with biotin-conjugated cello-oligosaccharides

The biotin-conjugated nonwovens after washing with DMSO were immersed in 1 mL of PBS for 25 min during which the PBS was refreshed every five minutes. The biotin-conjugated nonwovens impregnated with PBS were immersed in 500 μL of 3% BSA/PBS solution containing HRP-conjugated anti-biotin IgG (or anti-mouse IgG IgG) at an IgG concentration of 100 ng mL⁻¹ (unless otherwise stated) at room temperature for 10 min. Free IgG molecules in the bulk solutions were removed by immersing the nonwovens in 1 mL of PBS for 25 min during which the PBS was refreshed every five minutes. The washed nonwovens were immersed in 500 μL of McIlvaine buffer solution (pH 4.0) containing 2 mg mL⁻¹ *o*-phenylenediamine (OPD) and 0.03% (v/v) H₂O₂ at room temperature for 10 min to allow the HRP-catalyzed reaction to occur. Then, 3 M H₂SO₄ aqueous solution was added to stop the catalytic reaction. A microplate reader (Model 680, Bio-Rad Laboratories, California, U.S.A.) was used to record the absorbance at 490 nm for 100 μL of the reaction solution in a 96-well plate at room temperature. The contribution of spontaneous reactions of OPD was subtracted from the measured absorbance.

To evaluate the intrinsic activities of HRP conjugated to anti-biotin IgG or anti-mouse IgG IgG, 200 μL of the OPD solution containing H₂O₂ was added to 8 μL of 3% BSA/PBS solutions containing the IgGs at 0, 20, 40, 60, 80, and 100 ng mL⁻¹. After 10 min, the enzymatic reactions were stopped by adding 200 μL of 3 M H₂SO₄ aqueous solution, and the absorbance at 490 nm of the solutions was recorded using

a microplate reader (Model 680, Bio-Rad Laboratories, California, U.S.A.).

3. Results and discussion

3.1. Self-assembly of azidated cello-oligosaccharides in polyolefin nonwovens

We firstly investigated the neutralization-induced self-assembly of azidated cello-oligosaccharides in IPA aqueous solutions in the absence of nonwoven fabrics because hydrophobic nonwoven fabrics were found to be impermeable to water (see below). Azidated cello-oligosaccharides used in this study were synthesized via the CDP-catalyzed oligomerization, according to the procedure described in our previous report (Figure S1) [33]. Their oligosaccharide moieties had an average DP of ~ 7 . When azidated cello-oligosaccharides were subjected to the neutralization-induced self-assembly, they successfully self-assembled and formed gels irrespective of the presence of IPA (Figure S2(a)). The average DP of oligosaccharide moieties and molecular weight distribution hardly changed through the self-assembly in the presence of IPA (Figure S2(b,c)). The assembled oligosaccharides were in the cellulose II allomorph, which is the thermodynamically most stable allomorph for cellulose; FTIR absorption spectra showed peaks at $\sim 3,440$ and 3490 cm^{-1} , assignable to the intrachain hydrogen-bonded hydroxy groups in the cellulose II allomorph (Figure S2(d)) [36]. The assembled gels were composed of nanoribbon-shaped fibers, which were considered to be lamellar crystals of the oligosaccharides (Figure S3) [37]. Cello-oligosaccharides without azido group self-assembled in IPA aqueous solutions as well (Figure S4). Nevertheless, it was found that the introduction of an azido group at the terminal end and the presence of IPA increased the self-assembly kinetics of the oligosaccharide molecules (Figure S5). Water – IPA mixtures appeared to be poorer solvents for cello-oligosaccharides. These results show that azidated cello-oligosaccharides can self-assemble even in the presence of IPA, albeit with faster kinetics.

Azidated cello-oligosaccharides were allowed to self-assemble in polyolefin nonwoven fabrics. The alkaline solutions of the oligosaccharides were applied to polyolefin nonwoven fabrics impregnated with HCl solutions (Figure 2(a)). Although the solutions without IPA remained as droplets on the hydrophobic nonwoven surfaces, the application of IPA to nonwovens prior to the oligosaccharide solution application allowed the aqueous solutions to permeate the hydrophobic nonwoven fabrics. After self-assembly, the rates of azidated cello-oligosaccharides loaded into nonwovens were estimated (Figure 2(b)). It was found that IPA at 5% (v/v) or higher concentrations facilitated the loading of oligosaccharides into nonwovens. The

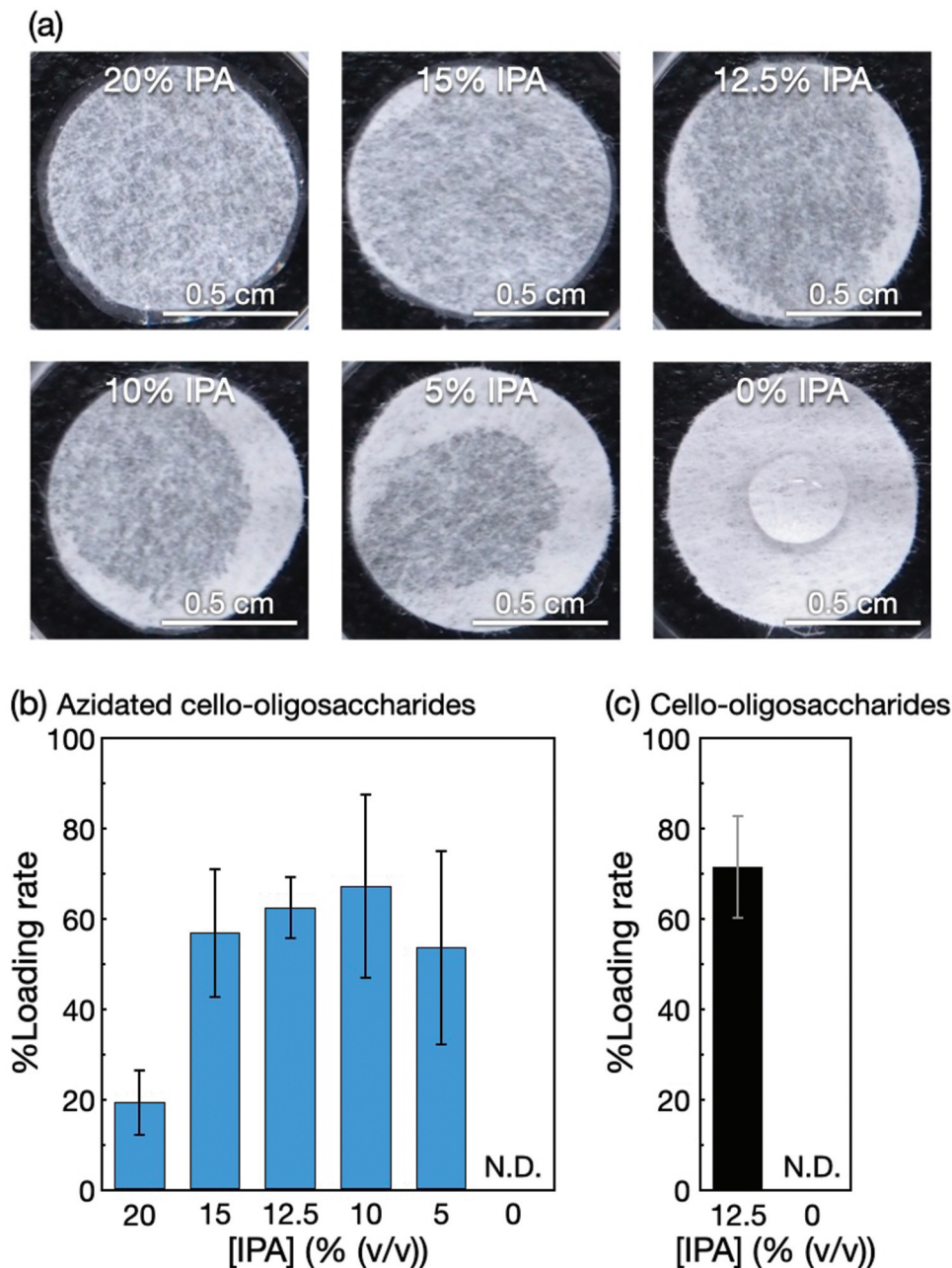


Figure 2. Self-assembly of azidated cello-oligosaccharides in polyolefin nonwoven with IPA. (a) Photographs of polyolefin nonwovens impregnated with different concentrations of IPA aqueous solutions containing 1% (w/v) azidated cello-oligosaccharides. Loading rates of (b) azidated cello-oligosaccharides and (c) cello-oligosaccharides into polyolefin nonwovens at different IPA concentrations. The loading rate values are presented as the average of nine individual trials, and the error bars represent the standard deviation of those trials.

loading rates were almost constant for IPA concentrations ranging from 5 to 15% (v/v). The 20% (v/v) IPA yielded a lower loading rate. This was attributed to the faster self-assembly kinetics of azidated cello-oligosaccharides in the presence of IPA (Figure S5(a)), which potentially increased the frequency of homogeneous nucleation in the bulk solution. The optimal IPA concentration for the loading of azidated cello-oligosaccharides with relatively high reproducibility was 12.5% (v/v) (Figure 2(b)). At this IPA concentration, cello-oligosaccharides without azido group could be loaded into polyolefin nonwovens as well

(Figure 2(c)). These results show that the neutralization-induced self-assembly using IPA aqueous solutions enables us to load azidated cello-oligosaccharides and cello-oligosaccharides into hydrophobic nonwovens.

3.2. Characterizations of polyolefin nonwovens with azidated cello-oligosaccharides

The polyolefin nonwovens with azidated cello-oligosaccharides (Figure 3(a)) were structurally characterized. SEM observations revealed that the surfaces of nonwoven microfibers with self-assembled azidated

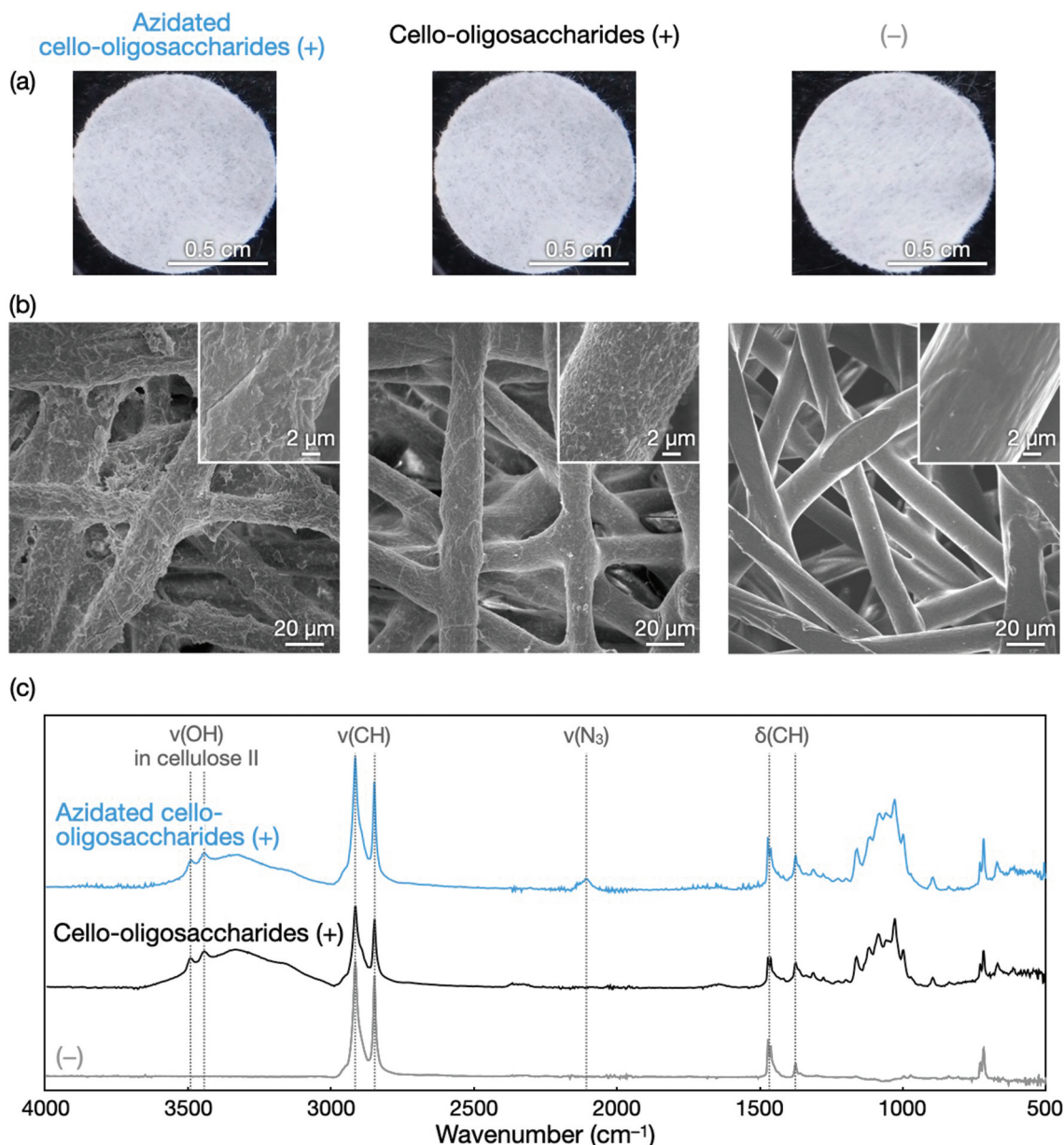


Figure 3. Structural characterization of azidated cello-oligosaccharide-decorated polyolefin nonwovens. (a) Photographs, (b) SEM images, and (c) ATR-FTIR absorption spectra of polyolefin nonwovens with and without azidated cello-oligosaccharides and cello-oligosaccharides.

cello-oligosaccharides and cello-oligosaccharides were rough and bark-like (Figure 3(b)). These surface structures were different from the smooth surfaces of nonwovens without oligosaccharides. These results indicate that the surface structures were assemblies of the oligosaccharides, and consequently, that oligosaccharide self-assembly enabled the decoration of nonwoven microfiber surfaces. It appears that the azidated cello-oligosaccharide assemblies were rougher than the cello-oligosaccharide assemblies, suggesting that the terminal azido group altered the oligosaccharide self-assembly behavior onto polyolefin surfaces. Notably, the bark-like structures of the oligosaccharide assemblies on polyolefin nonwoven surfaces were different from the hairy structures of the azidated cello-oligosaccharide assemblies formed on paper microfibers [33]. It seems that the differences

in the polymer species constituting microfibers (polyolefin and cellulose for nonwoven and paper, respectively) and the solvents (12.5% (v/v) IPA aqueous solutions and water for nonwoven and paper, respectively) affected the assembled structures of azidated cello-oligosaccharides. Moreover, the bark-like structures were significantly different from the nanoribbon networks formed in bulk solutions (Figure S3), indicating that oligosaccharide self-assembly was mediated by polymer surfaces.

FTIR absorption spectra of the azidated cello-oligosaccharide-decorated polyolefin nonwovens showed peaks corresponding to azido group at $\sim 2,100\text{ cm}^{-1}$ [38], indicating that azido groups were successfully introduced into the polyolefin nonwovens (Figure 3(c)). The nonwovens with azidated cello-oligosaccharides and those with cello-

oligosaccharides exhibited characteristic absorptions at $\sim 3,440$ and 3490 cm^{-1} assignable to the intrachain hydrogen-bonded hydroxy groups in the cellulose II allomorph [36]. This crystal allomorph is the thermodynamically most stable for cellulose and is the same as that of azidated cello-oligosaccharides assembled on paper microfibrers [33].

Water droplets were mounted onto the polyolefin nonwovens with and without the oligosaccharides. The contact angles of the water droplets were lower for the nonwovens with oligosaccharides than for those without oligosaccharides (Figure 4), demonstrating that the loading of oligosaccharides endowed the hydrophobic nonwovens with water wettability. It is noted that the nonwovens with azidated cello-oligosaccharides exhibited a lower contact angle than those with cello-oligosaccharides (Figure 4(b)). The t-test showed statistical significance for the difference ($p = 0.001$). Given the slightly lower loading rate for azidated cello-oligosaccharides (Figure 2(b,c)) and the higher hydrophobicity of azido group than hydroxy group [39], the rougher surfaces of the azidated cello-oligosaccharide-decorated nonwoven microfibrers (Figure 3(b)) seemed to contribute to the higher water wettability [40].

3.3. Modification of polyester and vinylon nonwovens

Other polymeric nonwovens, namely, polyester and vinylon nonwovens, were subjected to the modification with azidated cello-oligosaccharides. When azidated cello-oligosaccharides were allowed to self-assemble at 1% (w/v) in polyester and vinylon nonwovens with 12.5% (v/v) IPA, the loading rates of the oligosaccharides into nonwovens were several tens of percent (Figure 5(a,b)). The use of IPA increased the loading rate. SEM observations revealed bark-like morphologies of the nonwoven microfiber surfaces (Figure 5(c,d)). Given the smooth surfaces of raw nonwovens (Figure S6), the azidated cello-oligosaccharide assemblies appeared to cover the microfiber surfaces. It is noted that the morphologies of the oligosaccharide assemblies varied depending on polymer species (Figures 3(b) and 5(c,d)), suggesting that oligosaccharide self-assembly was mediated by the polymer surface properties (e.g. hydrophobicity). ATR-FTIR absorption spectra showed that azido groups were successfully introduced into polyester and vinylon nonwovens and that the cello-oligosaccharide moieties in the

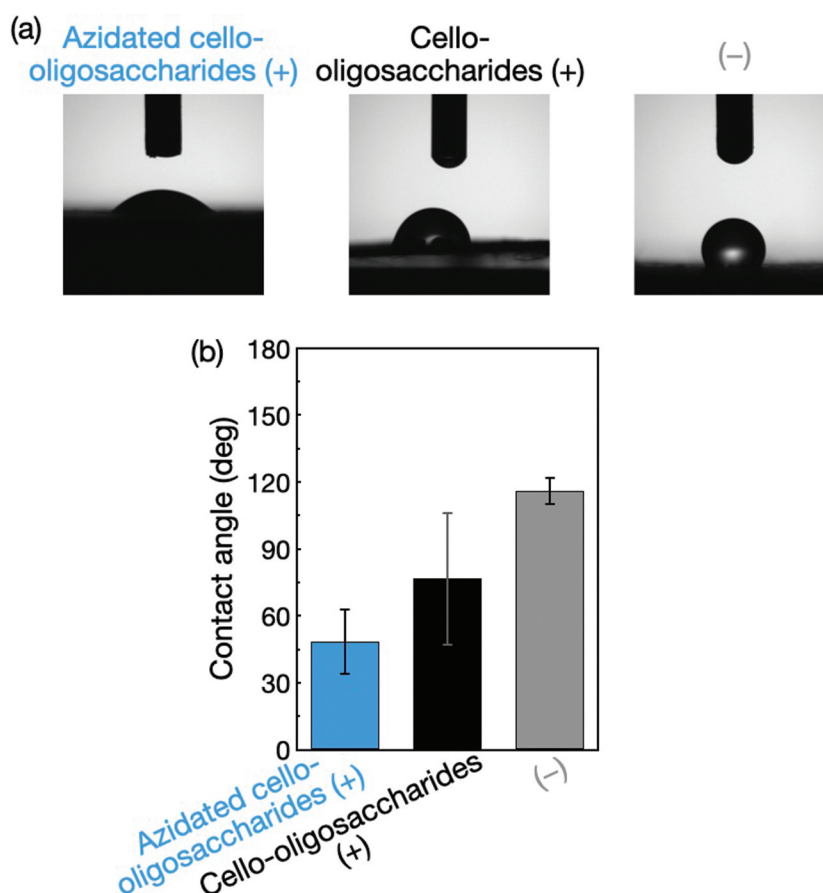


Figure 4. Contact angle measurements for the surface-modified polyolefin nonwovens. (a) Photographs and (b) Contact angles of water droplets on the polyolefin nonwovens with and without azidated cello-oligosaccharides and cello-oligosaccharides. The contact angle values are presented as the average of nine individual trials, and the error bars represent the standard deviation of those trials.

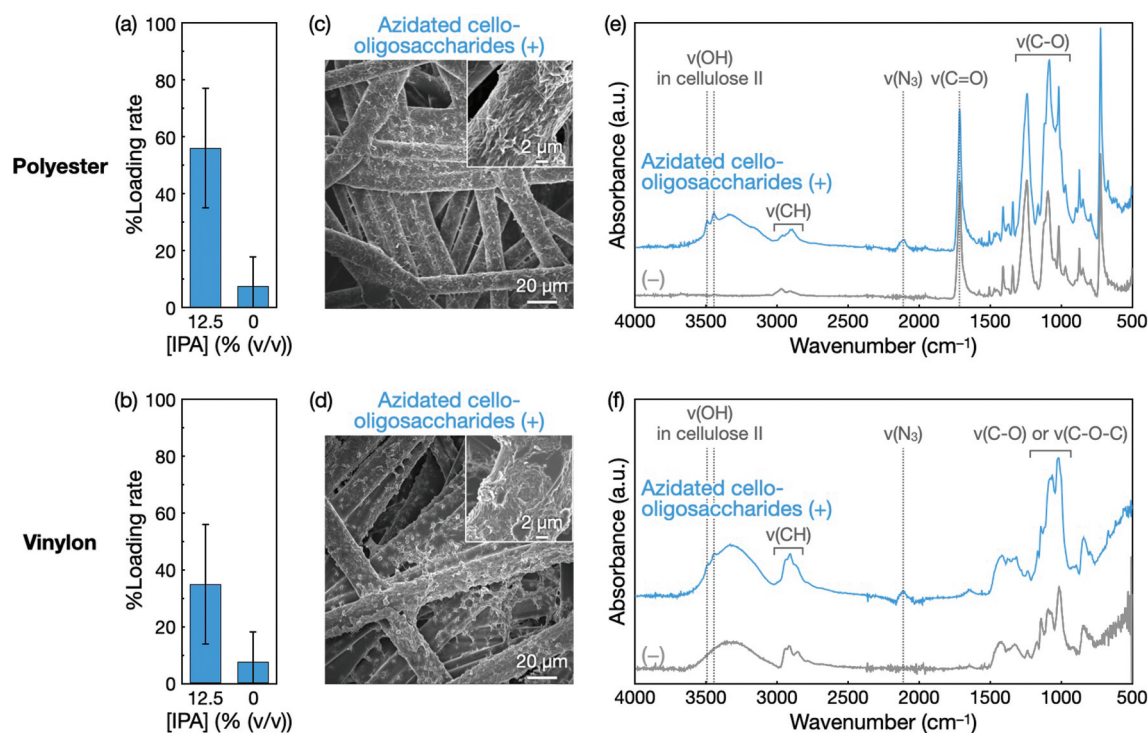


Figure 5. Self-assembly of azidated cello-oligosaccharides at 1% (w/v) in polyester and vinylon nonwovens with IPA. Loading rates of azidated cello-oligosaccharides into (a) polyester and (b) vinylon nonwovens. The loading rate values are presented as the average of nine individual trials, and the error bars represent the standard deviation of those trials. SEM images of (c) polyester and (d) vinylon nonwovens with azidated cello-oligosaccharides. ATR-FTIR absorption spectra of (e) polyester and (f) vinylon nonwovens with and without azidated cello-oligosaccharides.

assemblies on nonwovens were in the cellulose II allomorph (Figure 5(e,f)). These results demonstrate that the surface modification via the self-assembly of azidated cello-oligosaccharides is applicable to various polymeric nonwovens.

3.4. Conjugation of an antigen via the click reaction

We hypothesized that the hydrophilic and click-reactive nonwovens decorated with azidated cello-oligosaccharides could be useful for developing biomolecular sensing platforms. This potential was investigated through a model experiment where a target antibody, HRP-conjugated anti-biotin IgG, was detected using biotin. Specifically, the small-molecule antigen, biotin, was conjugated to the click-reactive nonwovens, and the resultant biotinylated nonwovens were used to detect anti-biotin IgG.

Alkynylated biotin was synthesized (Figure S7) and applied to the polyolefin nonwovens with azidated cello-oligosaccharides (Figure 6(a)). After the click reaction in 50% DMSO, the oligosaccharides in nonwovens were extracted using alkali solutions and subjected to MALDI-TOF mass spectrometry measurements. The mass spectra showed a series of peaks corresponding to the cello-oligosaccharides conjugated with biotin via the click reaction

(Figure 6(b)). The rate of biotin conjugation to azidated cello-oligosaccharides in nonwovens was estimated from the mass spectra to be $24.5 \pm 1.9\%$, which was comparable to the biotin conjugation rate for the azidated cello-oligosaccharide-decorated paper ($\sim 20\%$) [33]. This conjugation rate is low for click reactions and is attributed to the possibility that the linker-conjugated biotin molecules were unaccessible to a large portion of the azido groups in the assemblies. Given that the assemblies had bark-like structures at the submicro- and micrometer scales (Figure 3(b)), a large portion of the azido groups seemed to be embedded in the submicro- and microstructures. It is emphasized that the analysis by MALDI-TOF mass spectrometry is exceptional for modified nonwovens. It is generally difficult to quantify the amount of functional moieties introduced into nonwovens. On the other hand, the chemical conjugation of functional moieties to the oligosaccharide-decorated nonwovens can be precisely analyzed *ex situ* at the molecular level (Figure 6(b)).

3.5. Detection of IgG

The biotinylated polyolefin nonwoven was used for the detection of anti-biotin IgG. Notably, the water wettability of oligosaccharide-decorated nonwovens enabled us to perform detection procedure in fully

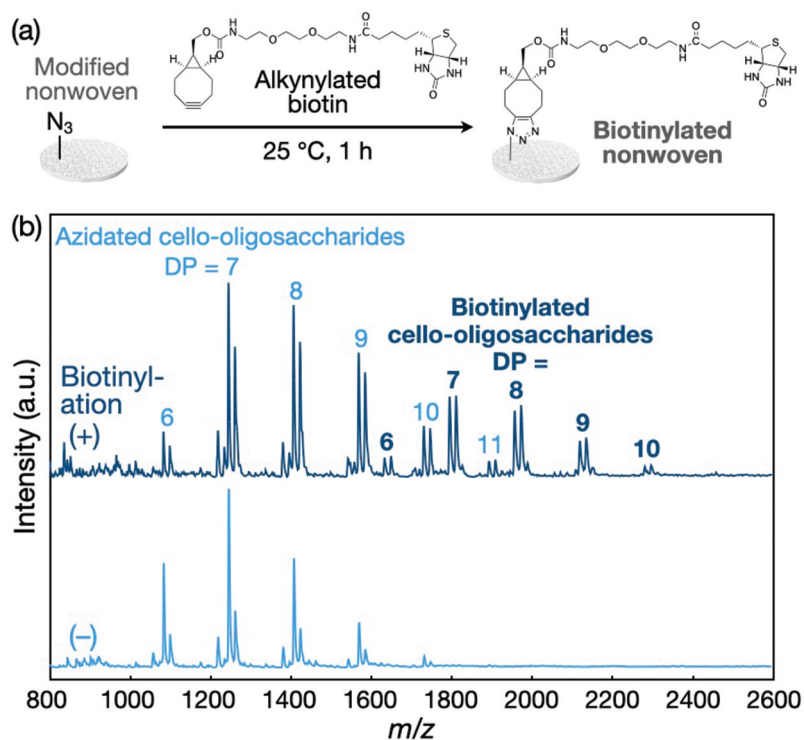


Figure 6. Conjugation of biotin to the polyolefin nonwoven with azidated cello-oligosaccharides via the click reaction. (a) Scheme for the conjugation. (b) MALDI-TOF mass spectra of azidated cello-oligosaccharides in the nonwovens before and after biotinylation.

aqueous media. Moreover, the assembled state of oligosaccharides on nonwoven surfaces was stable and remained throughout the process, from the click reaction in 50% DMSO and subsequent repetitive washing with DMSO to the IgG detection that required H_2O_2 .

HRP-conjugated anti-biotin IgG was applied at 100 ng mL^{-1} to the biotinylated nonwoven, followed by the HRP-catalyzed conversion of OPD with H_2O_2 into a dye, 2,3-diaminophenazine (Figure 7(a)). Figure 7(b) shows the absorbance derived from the dye corresponding to the relative amounts of anti-biotin IgG adsorbed on the biotinylated nonwovens and control samples. The biotinylated nonwovens yielded an absorbance value much higher than those of nonwovens without azidated cello-oligosaccharides after treatment with alkyne-biotin (see the leftmost two bars) and nonwovens with and without azidated cello-oligosaccharides (i.e. without alkyne-biotin, the rightmost two bars), indicating that the detection of anti-biotin IgG was successful and that anti-biotin IgG was adsorbed onto the biotinylated polyolefin nonwoven through the specific antigen-antibody interaction. Notably, the absorbance value with chemically conjugated biotin via azidated cello-oligosaccharides was ~ 12 -fold higher than that with physically adsorbed biotin without azidated cello-oligosaccharides (the leftmost two bars); this difference was greater than the previously reported ~ 6 -fold difference using biotinylated paper [33]. Azidated cello-oligosaccharide-decorated nonwovens treated with biotin (not alkyne-biotin)

yielded a lower but substantial absorbance value, even though nonwovens treated with biotin yielded negligible absorbance (see the middle two bars). The azidated cello-oligosaccharide assemblies may physically adsorb biotin for subsequent adsorption of anti-biotin IgG.

When anti-mouse IgG IgG, which does not bind to biotin, was used instead of anti-biotin IgG, absorbance values remained negligible even for the biotinylated nonwovens (Figure 7(c)). It is mentioned that the catalytic activity of HRP conjugated to anti-mouse IgG IgG was $\sim 20\%$ lower than that of HRP conjugated to anti-biotin IgG (Figure S8), indicating a slight underestimation of the amount of anti-mouse IgG IgG adsorbed on nonwovens. Nevertheless, the difference in the absorbance values for anti-biotin IgG and anti-mouse IgG IgG was significant. In fact, when IgG concentrations were varied, the absorbance increased linearly with increasing IgG concentrations, and the slope for anti-biotin IgG was more than 40-fold higher than that for anti-mouse IgG IgG (Figure 7(d)). This result demonstrates that the detection of anti-biotin IgG using the biotinylated nonwovens was quantitative and specific.

The polyester nonwovens with biotinylated cello-oligosaccharides were also available for the specific detection of anti-biotin IgG (Figure S9). Given that the antigen (biotin) was introduced into the nonwovens via click chemistry, various antigens will readily be introduced into nonwovens decorated with azidated cello-oligosaccharides. Collectively, the self-assembly of azidated cello-

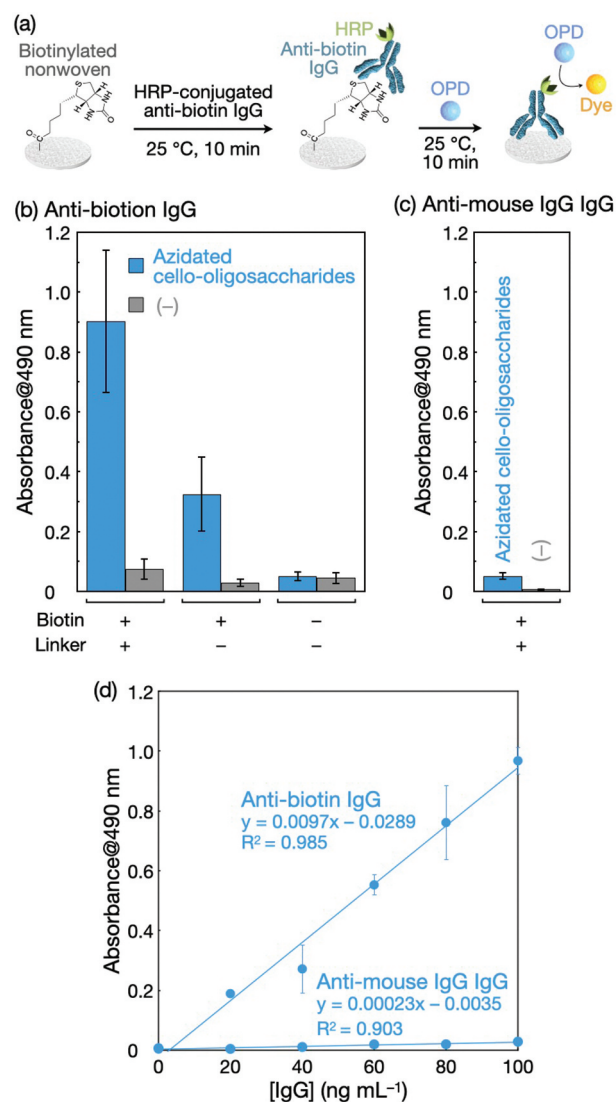


Figure 7. The detection of anti-biotin IgG using the biotinylated polyolefin nonwoven. (a) Scheme for the IgG detection. Absorbance at 490 nm of the HRP-catalyzed reaction products from (b) HRP-conjugated anti-biotin IgG and (c) HRP-conjugated anti-mouse IgG adsorbed on the biotinylated nonwoven and control samples. IgGs were applied at 100 ng mL⁻¹ to nonwovens. The leftmost bars in (b) and (c) (azidated cello-oligosaccharides with biotin (+) and linker (+)) represent the results for the biotinylated nonwovens, and 'linker' denotes BCN-amine. The absorbance values are presented as the average of nine individual trials, and the error bars represent the standard deviation of those trials. (d) Effect of IgG concentration on absorbance at 490 nm for detection. The absorbance values are presented as the average of three individual trials, and the error bars represent the standard deviation of those trials.

oligosaccharides is a promising strategy for converting conventional nonwoven fabrics into versatile biomolecular sensing platforms.

4. Conclusions

We have presented the modification of polymer nonwoven fabrics via the surface-mediated self-assembly of azidated cello-oligosaccharides. The

azidated cello-oligosaccharide assemblies were stable not only on cellulose surfaces [33,34], which had identical chemical structures, but also on the polyolefin, polyester, and vinylon surfaces, demonstrating the versatility of this surface functionalization method. This remarkable characteristic of azidated cello-oligosaccharide assemblies can be attributed to the amphiphilic nature [41–43] and the strong intermolecular interactions [44] of cello-oligosaccharides [20,21]. Another advantage of cello-oligosaccharides is that their derivatives with various terminal groups, such as amino [45], vinyl [46], thiol [47,48], phenolic [49], oligo(ethylene glycol) [50], and alkyl groups [51], are readily synthesized via the CDP-catalyzed oligomerization using glucose derivative primers. Their use should allow the introduction of various functions into polymer fabrics. Moreover, there are many types of candidate self-assembling building blocks [52–58]. Taken together, surface-mediated self-assembly will be a versatile strategy for the modification of fabrics and other polymeric materials.

Acknowledgments

The authors thank Mr. M. Nishiura, Ms. R. Murase, and Ms. N. Hayakawa (DKS Co. Ltd.) for cooperative research and fruitful discussions and the Materials Analysis Division, Open Facility Center (Tokyo Tech) for SEM observations.

Disclosure statement

No potential conflict of interest was reported by the author(s).

Funding

The authors are grateful for financial support from a Grants-in-Aid for Scientific Research from the Japan Society for the Promotion of Science (JSPS) [JP21H01996] to T. Serizawa, a Grant-in-Aid for Early-Career Scientists from JSPS [JP21K14688] to Y.H., and Grants-in-Aid for Scientific Research on Innovative Areas (Aquatic Functional Materials) from the Ministry of Education, Culture, Sports, Science and Technology, Japan [JP22H04528] to T. Serizawa.

ORCID

Yuuki Hata <http://orcid.org/0000-0003-1493-1896>
Toshiki Sawada <http://orcid.org/0000-0001-7491-8357>
Takeshi Serizawa <http://orcid.org/0000-0002-4867-8625>

References

- [1] Rao YS, Mohan NS, Shetty N, et al. Drilling and structural property study of multi-layered fiber and fabric reinforced polymer composite – a review.

- Mater Manuf Process. 2019;34(14):1549–1579. doi: [10.1080/10426914.2019.1686522](https://doi.org/10.1080/10426914.2019.1686522)
- [2] Jabbour CR, Parker LA, Hutter EM, et al. Chemical targets to deactivate biological and chemical toxins using surfaces and fabrics. *Nat Rev Chem*. 2021;5(6):370–387. doi: [10.1038/s41570-021-00275-4](https://doi.org/10.1038/s41570-021-00275-4)
- [3] Xiong J, Chen J, Lee PS. Functional fibers and fabrics for soft robotics, wearables, and human–robot interface. *Adv Mater*. 2021;33(19):2002640. doi: [10.1002/adma.202002640](https://doi.org/10.1002/adma.202002640)
- [4] Ali AE, Jeoti V, Stojanović GM. Fabric based printed-distributed battery for wearable e-textiles: a review. *Sci Technol Adv Mater*. 2021;22(1):772–793. doi: [10.1080/14686996.2021.1962203](https://doi.org/10.1080/14686996.2021.1962203)
- [5] Dong K, Peng X, Cheng R, et al. Advances in high-performance autonomous energy and self-powered sensing textiles with novel 3D fabric structures. *Adv Mater*. 2022;34(21):2109355. doi: [10.1002/adma.202109355](https://doi.org/10.1002/adma.202109355)
- [6] Ishihara K. Biomimetic materials based on zwitterionic polymers toward human-friendly medical devices. *Sci Technol Adv Mater*. 2022;23(1):498–524. doi: [10.1080/14686996.2022.2119883](https://doi.org/10.1080/14686996.2022.2119883)
- [7] Vohrer U. Interfacial engineering of functional textiles for biomedical applications. In: Shishoo R, editor. *Plasma technologies for textiles: a volume in woodhead publishing series in textiles*. Cambridge: Woodhead Publishing Limited; 2007. p. 202–227.
- [8] Xiang B, Liu Q, Sun Q, et al. Recent advances in eco-friendly fabrics with special wettability for oil/water separation. *Chem Commun*. 2022;58(97):13413–13438. doi: [10.1039/D2CC05780H](https://doi.org/10.1039/D2CC05780H)
- [9] Zhang M, Chu L, Chen J, et al. Asymmetric wettability fibrous membranes: preparation and biologic applications. *Compos B Eng*. 2024;269:111095. doi: [10.1016/j.compositesb.2023.111095](https://doi.org/10.1016/j.compositesb.2023.111095)
- [10] Wang W, Feng L, Song B, et al. Fabrication and application of superhydrophobic nonwovens: a review. *Mater Today Chem*. 2022;26:101227. doi: [10.1016/j.mtchem.2022.101227](https://doi.org/10.1016/j.mtchem.2022.101227)
- [11] Ren F, He R, Ren J, et al. A friendly UV-responsive fluorine-free superhydrophobic coating for oil-water separation and dye degradation. *Bull Chem Soc Jpn*. 2022;95(7):1091–1099. doi: [10.1246/bcsj.20220042](https://doi.org/10.1246/bcsj.20220042)
- [12] Shishoo R. *Plasma technologies for textiles*. Cambridge: Woodhead Publishing Limited; 2007.
- [13] Nemani SK, Annavarapu RK, Mohammadian B, et al. Surface modification of polymers: methods and applications. *Adv Mater Interfaces*. 2018;5(24):1801247. doi: [10.1002/admi.201801247](https://doi.org/10.1002/admi.201801247)
- [14] Kowalczyk T. Functional micro- and nanofibers obtained by nonwoven post-modification. *Polymers*. 2020;12(5):1087. doi: [10.3390/polym12051087](https://doi.org/10.3390/polym12051087)
- [15] Yamamoto K, Asahara H, Moriguchi M, et al. Immobilization of β -cyclodextrin onto polypropylene nonwoven fabric based on photooxidative surface modification. *Polym J*. 2023;55(5):599–605. doi: [10.1038/s41428-022-00751-8](https://doi.org/10.1038/s41428-022-00751-8)
- [16] Gu J, Xiao P, Chen P, et al. Functionalization of biodegradable PLA nonwoven fabric as superoleophilic and superhydrophobic material for efficient oil absorption and oil/water separation. *ACS Appl Mater Interfaces*. 2017;9(7):5968–5973. doi: [10.1021/acsami.6b13547](https://doi.org/10.1021/acsami.6b13547)
- [17] Xiao X, Chen F, Wei Q, et al. Surface modification of polyester nonwoven fabrics by Al_2O_3 sol–gel coating. *J Coat Technol Res*. 2009;6(4):537–541. doi: [10.1007/s11998-008-9157-x](https://doi.org/10.1007/s11998-008-9157-x)
- [18] Shen L, Wang X, Zhang Z, et al. Design and fabrication of the evolved zeolitic imidazolate framework-modified polylactic acid nonwoven fabric for efficient oil/water separation. *ACS Appl Mater Interfaces*. 2021;13(12):14653–14661. doi: [10.1021/acsami.0c22090](https://doi.org/10.1021/acsami.0c22090)
- [19] Zhu C, Jiang W, Hu J, et al. Polylactic acid nonwoven fabric surface modified with stereocomplex crystals for recyclable use in oil/water separation. *ACS Appl Polym Mater*. 2020;2(7):2509–2516. doi: [10.1021/acsapm.9b01197](https://doi.org/10.1021/acsapm.9b01197)
- [20] Hata Y, Serizawa T. Self-assembly of cellulose for creating green materials with tailor-made nanostructures. *J Mater Chem B*. 2021;9(19):3944–3966. doi: [10.1039/d1tb00339a](https://doi.org/10.1039/d1tb00339a)
- [21] Hata Y, Serizawa T. Robust gels composed of self-assembled cello-oligosaccharide networks. *Bull Chem Soc Jpn*. 2021;94(9):2279–2289. doi: [10.1246/bcsj.20210234](https://doi.org/10.1246/bcsj.20210234)
- [22] Hata Y, Sawada T, Sakai T, et al. Enzyme-catalyzed bottom-up synthesis of mechanically and physico-chemically stable cellulose hydrogels for spatial immobilization of functional colloidal particles. *Biomacromolecules*. 2018;19(4):1269–1275. doi: [10.1021/acs.biomac.8b00092](https://doi.org/10.1021/acs.biomac.8b00092)
- [23] Hata Y, Saito Y, Sawada T, et al. Assembly of reduced graphene oxides into a three-dimensional porous structure via confinement within robust cellulose oligomer networks. *RSC Adv*. 2019;9(66):38848–38854. doi: [10.1039/c9ra08318a](https://doi.org/10.1039/c9ra08318a)
- [24] Hata Y, Sawada T, Serizawa T. Confined reduced graphene oxides as a platform for DNA sensing in solutions crowded with biomolecules. *ACS Appl Bio Mater*. 2020;3(5):3210–3216. doi: [10.1021/acsabm.0c00206](https://doi.org/10.1021/acsabm.0c00206)
- [25] Buffiere J, Balogh-Michels Z, Borrega M, et al. The chemical-free production of nanocelluloses from microcrystalline cellulose and their use as Pickering emulsion stabilizer. *Carbohydr Polym*. 2017;178:48–56. doi: [10.1016/j.carbpol.2017.09.028](https://doi.org/10.1016/j.carbpol.2017.09.028)
- [26] Yataka Y, Tanaka S, Sawada T, et al. Mechanically robust crystalline monolayer assemblies of oligosaccharide-based amphiphiles on water surfaces. *Chem Commun*. 2019;55(76):11346–11349. doi: [10.1039/c9cc05629g](https://doi.org/10.1039/c9cc05629g)
- [27] Hata Y, Yoneda S, Tanaka S, et al. Structured liquids with interfacial robust assemblies of a nonionic crystalline surfactant. *J Colloid Interface Sci*. 2021;590:487–494. doi: [10.1016/j.jcis.2021.01.064](https://doi.org/10.1016/j.jcis.2021.01.064)
- [28] Serizawa T, Maeda T, Sawada T. Neutralization-induced self-assembly of cellulose oligomers into antibiofouling crystalline nanoribbon networks in complex mixtures. *ACS Macro Lett*. 2020;9(3):301–305. doi: [10.1021/acsmacrolett.9b01008](https://doi.org/10.1021/acsmacrolett.9b01008)
- [29] Serizawa T, Maeda T, Yamaguchi S, et al. Aqueous suspensions of cellulose oligomer nanoribbons for growth and natural filtration-based separation of cancer spheroids. *Langmuir*. 2020;36(46):13890–13898. doi: [10.1021/acs.langmuir.0c02294](https://doi.org/10.1021/acs.langmuir.0c02294)
- [30] Song J, Li Q, Miao W, et al. In situ preparation and properties of polyvinyl alcohol/synthetic ribbon-like nanocellulose composites. *Int J Biol Macromol*. 2024;254:127517. doi: [10.1016/j.ijbiomac.2023.127517](https://doi.org/10.1016/j.ijbiomac.2023.127517)
- [31] Sugiura K, Sawada T, Hata Y, et al. Distinguishing anti-PEG antibodies by specificity for the PEG terminus using nanoarchitectonics-based antibiofouling

- cello-oligosaccharide platforms. *J Mater Chem B*. 2024;12(3):650–657. doi: [10.1039/D3TB01723K](https://doi.org/10.1039/D3TB01723K)
- [32] Serizawa T, Yamaguchi S, Sugiura K, et al. Antibacterial synthetic nanocelluloses synergizing with a metal-chelating agent. *ACS Appl Bio Mater*. 2024;7(1):246–255. doi: [10.1021/acsabm.3c00846](https://doi.org/10.1021/acsabm.3c00846)
- [33] Hanamura M, Sawada T, Serizawa T. In-paper self-assembly of cellulose oligomers for the preparation of all-cellulose functional paper. *ACS Sustainable Chem Eng*. 2021;9(16):5684–5692. doi: [10.1021/acsuschemeng.1c00815](https://doi.org/10.1021/acsuschemeng.1c00815)
- [34] Hata Y, Hiruma S, Sakurai Y, et al. Nanospiked paper: microfibrillar cellulose materials nanostructured via partial hydrolysis and self-assembly. *Carbohydr Polym*. 2023;300:120257. doi: [10.1016/j.carbpol.2022.120257](https://doi.org/10.1016/j.carbpol.2022.120257)
- [35] Sugiura K, Saito M, Sawada T, et al. Cellodextrin phosphorylase-catalyzed single-process production and superior mechanical properties of organic-inorganic hybrid hydrogels composed of surface-carboxylated synthetic nanocelluloses and hydroxyapatite. *ACS Sustainable Chem Eng*. 2022;10(40):13484–13494. doi: [10.1021/acssuschemeng.2c04349](https://doi.org/10.1021/acssuschemeng.2c04349)
- [36] Hishikawa Y, Togawa E, Kondo T. Characterization of individual hydrogen bonds in crystalline regenerated cellulose using resolved polarized FTIR spectra. *ACS Omega*. 2017;2(4):1469–1476. doi: [10.1021/acsomega.6b00364](https://doi.org/10.1021/acsomega.6b00364)
- [37] Serizawa T, Fukaya Y, Sawada T. Self-assembly of cellulose oligomers into nanoribbon network structures based on kinetic control of enzymatic oligomerization. *Langmuir*. 2017;33(46):13415–13422. doi: [10.1021/acs.langmuir.7b03653](https://doi.org/10.1021/acs.langmuir.7b03653)
- [38] Yarlagadda V, Konai MM, Manjunath GB, et al. Tackling vancomycin-resistant bacteria with 'lipophilic–vancomycin–carbohydrate conjugates'. *J Antibiot*. 2015;68(5):302–312. doi: [10.1038/ja.2014.144](https://doi.org/10.1038/ja.2014.144)
- [39] Ha S, Kim KT. Effect of hydrophilic block end groups and block junction on block copolymer self-assembly in solution. *RSC Adv*. 2022;12(12):7446–7452. doi: [10.1039/D2RA00493C](https://doi.org/10.1039/D2RA00493C)
- [40] Wenzel RN. Resistance of solid surfaces to wetting by water. *Ind Eng Chem*. 1936;28(8):988–994. doi: [10.1021/ie50320a024](https://doi.org/10.1021/ie50320a024)
- [41] Yamane C, Aoyagi T, Ago M, et al. Two different surface properties of regenerated cellulose due to structural anisotropy. *Polym J*. 2006;38(8):819–826. doi: [10.1295/polymj.PJ2005187](https://doi.org/10.1295/polymj.PJ2005187)
- [42] Miyamoto H, Umemura M, Aoyagi T, et al. Structural reorganization of molecular sheets derived from cellulose II by molecular dynamics simulations. *Carbohydr Res*. 2009;344(9):1085–1094. doi: [10.1016/j.carres.2009.03.014](https://doi.org/10.1016/j.carres.2009.03.014)
- [43] Lindman B, Medronho B, Alves L, et al. The relevance of structural features of cellulose and its interactions to dissolution, regeneration, gelation and plasticization phenomena. *Phys Chem Chem Phys*. 2017;19(35):23704–23718. doi: [10.1039/c7cp02409f](https://doi.org/10.1039/c7cp02409f)
- [44] Glasser WG, Atalla RH, Blackwell J, et al. About the structure of cellulose: debating the Lindman hypothesis. *Cellul*. 2012;19(3):589–598. doi: [10.1007/s10570-012-9691-7](https://doi.org/10.1007/s10570-012-9691-7)
- [45] Nohara T, Sawada T, Tanaka H, et al. Enzymatic synthesis and protein adsorption properties of crystalline nanoribbons composed of cellulose oligomer derivatives with primary amino groups. *J Biomater Sci Polym Ed*. 2017;28(10–12):925–938. doi: [10.1080/09205063.2017.1322248](https://doi.org/10.1080/09205063.2017.1322248)
- [46] Wang J, Niu J, Sawada T, et al. A bottom-up synthesis of vinyl-cellulose nanosheets and their nanocomposite hydrogels with enhanced strength. *Biomacromolecules*. 2017;18(12):4196–4205. doi: [10.1021/acs.biomac.7b01224](https://doi.org/10.1021/acs.biomac.7b01224)
- [47] Zhong C, Zajki-Zechmeister K, Nidetzky B. Reducing end thiol-modified nanocellulose: bottom-up enzymatic synthesis and use for templated assembly of silver nanoparticles into biocidal composite material. *Carbohydr Polym*. 2021;260:117772. doi: [10.1016/j.carbpol.2021.117772](https://doi.org/10.1016/j.carbpol.2021.117772)
- [48] Zhong C, Nidetzky B. Precision synthesis of reducing-end thiol-modified cellulose enabled by enzyme selection. *Polym J*. 2022;54(4):551–560. doi: [10.1038/s41428-021-00599-4](https://doi.org/10.1038/s41428-021-00599-4)
- [49] Fang C, Shao T, Ji X, et al. High mechanical property and antibacterial poly (3-hydroxybutyrate-co-3-hydroxyvalerate)/functional enzymatically-synthesized cellulose biodegradable composite. *Int J Biol Macromol*. 2023;225:776–785. doi: [10.1016/j.ijbiomac.2022.11.140](https://doi.org/10.1016/j.ijbiomac.2022.11.140)
- [50] Nohara T, Sawada T, Tanaka H, et al. Enzymatic synthesis of oligo(ethylene glycol)-bearing cellulose oligomers for in situ formation of hydrogels with crystalline nanoribbon network structures. *Langmuir*. 2016;32(47):12520–12526. doi: [10.1021/acs.langmuir.6b01635](https://doi.org/10.1021/acs.langmuir.6b01635)
- [51] Yataka Y, Sawada T, Serizawa T. Multidimensional self-assembled structures of alkylated cellulose oligomers synthesized via in vitro enzymatic reactions. *Langmuir*. 2016;32(39):10120–10125. doi: [10.1021/acs.langmuir.6b02679](https://doi.org/10.1021/acs.langmuir.6b02679)
- [52] Ariga K, Fakhruddin R. Materials nanoarchitectonics from atom to living cell: a method for everything. *Bull Chem Soc Jpn*. 2022;95(5):774–795. doi: [10.1246/bcsj.20220071](https://doi.org/10.1246/bcsj.20220071)
- [53] Liang J, Ouyang X, Cao Y. Interfacial and confined molecular-assembly of poly(3-hexylthiophene) and its application in organic electronic devices. *Sci Technol Adv Mater*. 2022;23(1):619–632. doi: [10.1080/14686996.2022.2125826](https://doi.org/10.1080/14686996.2022.2125826)
- [54] Hu W, Shi J, Lv W, et al. Regulation of stem cell fate and function by using bioactive materials with nanoarchitectonics for regenerative medicine. *Sci Technol Adv Mater*. 2022;23(1):393–412. doi: [10.1080/14686996.2022.2082260](https://doi.org/10.1080/14686996.2022.2082260)
- [55] Shen X, Song J, Sevencan C, et al. Bio-interactive nanoarchitectonics with two-dimensional materials and environments. *Sci Technol Adv Mater*. 2022;23(1):199–224. doi: [10.1080/14686996.2022.2054666](https://doi.org/10.1080/14686996.2022.2054666)
- [56] Yamamoto Y, Kushida S, Okada D, et al. Self-assembled π -conjugated organic/polymeric microresonators and microlasers. *Bull Chem Soc Jpn*. 2023;96(7):702–710. doi: [10.1246/bcsj.20230104](https://doi.org/10.1246/bcsj.20230104)
- [57] Roy B, Govindaraju T. Enzyme-mimetic catalyst architectures: the role of second coordination sphere in catalytic activity. *Bull Chem Soc Jpn*. 2023. doi: [10.1246/bcsj.20230224](https://doi.org/10.1246/bcsj.20230224)
- [58] Murai K. Development of peptide-inorganic hybrid materials based on biomineralization and their functional design based on structural controls. *Polym J*. 2023;55(8):817–827. doi: [10.1038/s41428-023-00783-8](https://doi.org/10.1038/s41428-023-00783-8)